

Prediction of Elastic-Airplane Longitudinal Dynamics from Rigid-Body Aerodynamics

Robert L. Swaim* and Donald G. Fullman†
Purdue University, West Lafayette, Ind.

Control-configured vehicle technology has increased the demand for detailed analysis of dynamic stability and control, handling and ride qualities, and control system dynamics at early stages of preliminary design. For these early analyses an approximate, but reasonably accurate, set of linear equations of motion for elastic airplanes is needed. Such a formulation is developed for the longitudinal dynamics of elastic airplanes. It makes use of rigid-body aerodynamic stability derivatives and the symmetric elastic mode shapes and frequencies in formulating the forces and moments caused by elastic motion. Verification of accuracy was made by comparison with B-1 airplane dynamics obtained by other methods. Frequencies and damping ratios of the coupled modes agree closely with four elastic modes included.

Nomenclature

| | | | |
|------------------------|--|--------------------|--|
| c | = mean aerodynamic chord, ft | M_{δ_e} | = aerodynamic pitching moment stability derivative because of elevator deflection, $1/\text{sec}^2$ |
| C_D | = drag coefficient | M_{ξ_i} | = aerodynamic pitching moment coefficient because of i th elastic mode generalized displacement, $\text{rad}/\text{ft}\cdot\text{sec}^2$ |
| C_{L_α} | = lift curve slope | $M_{\dot{\xi}_i}$ | = aerodynamic pitching moment coefficient because of i th elastic mode generalized velocity, $\text{rad}/\text{ft}\cdot\text{sec}$ |
| $C_{L_{\delta_e}}$ | = lift coefficient due to elevator deflection | $M_{\ddot{\xi}_i}$ | = aerodynamic pitching moment coefficient because of i th elastic mode generalized acceleration, rad/ft |
| C_{m_α} | = pitching moment coefficient because of angle of attack | \mathfrak{M}_i | = $\int_y \int_x m(x,y) \phi_i^2(x,y) dx dy$, i th elastic mode generalized mass, slugs |
| $C_{m_{\dot{\alpha}}}$ | = pitching moment coefficient because of rate of change of angle of attack | $q_g(t)$ | = pitch gust velocity, rad/sec |
| C_{m_q} | = pitching moment coefficient because of pitch rate | S or S_w | = wing planform reference area, ft^2 |
| $C_{m_{\delta_e}}$ | = pitching moment coefficient because of elevator deflection | S_{HT} | = horizontal tail planform reference area, ft^2 |
| F_{i_q} | = i th elastic mode aerodynamic force coefficient in z direction because of pitch rate, fps | U_0 | = trim flight velocity, fps |
| F_{i_w} | = i th elastic mode aerodynamic force coefficient in z direction because of plunge velocity of C.G., $1/\text{sec}$ | $w(x,y,t)$ | = local plunge velocity in z direction, fps |
| $F_{i_{\xi_j}}$ | = i th elastic mode aerodynamic force coefficient in z direction because of j th mode generalized displacement, $1/\text{sec}^2$ | $w_g(t)$ | = vertical gust velocity at C.G. in negative z direction, fps |
| $F_{i_{\dot{\xi}_j}}$ | = i th elastic mode aerodynamic force coefficient in z direction because of j th mode generalized velocity, $1/\text{sec}$ | Z_w | = aerodynamic force stability derivative in z direction because of plunge velocity of C.G., $1/\text{sec}$ |
| $F_{i_{\delta_e}}$ | = i th elastic mode aerodynamic force coefficient in z direction because of elevator deflection, ft/sec^2 | $Z_{\dot{w}}$ | = aerodynamic force stability derivative in z direction because of plunge acceleration of C.G. |
| $F_{i_{w_g}}$ | = i th elastic mode aerodynamic force coefficient in z direction because of vertical gust velocity, $1/\text{sec}$ | Z_{δ_e} | = aerodynamic force stability derivative in z direction because of elevator deflection, $\text{ft}/\text{rad}\cdot\text{sec}^2$ |
| I_y | = mass moment of inertia about y axis, slug/ft^2 | Z_q | = aerodynamic force stability derivative in z direction because of pitch rate, fps |
| M | = total airplane mass, slugs | Z_{ξ_i} | = aerodynamic force coefficient in z direction because of i th elastic mode generalized displacement, $1/\text{sec}^2$ |
| $m(x,y)$ | = mass per unit area, slug/ft^2 | $Z_{\dot{\xi}_i}$ | = aerodynamic force coefficient in z direction because of i th elastic mode generalized velocity, $1/\text{sec}$ |
| M_w | = aerodynamic pitching moment stability derivative because of plunge velocity of C.G., $\text{rad}/\text{ft}\cdot\text{sec}$ | $\alpha(x,y,t)$ | = local angle of attack, rad |
| $M_{\dot{w}}$ | = aerodynamic pitching moment stability derivative because of rate of change of angle of attack, rad/ft | δ_e | = elevator deflection, rad |
| M_q | = aerodynamic pitching moment stability derivative because of pitch rate, $1/\text{sec}$ | ξ_i | = i th elastic mode structural damping ratio |
| | | $\xi_i(t)$ | = i th elastic mode generalized displacement in z direction, ft |
| | | $\theta(x,y,t)$ | = local pitch angle, rad |
| | | ρ_0 | = freestream air density, slugs/ft^3 |
| | | ω_i | = free-free undamped natural frequency of i th elastic mode, rad/sec |
| | | $\phi_i(x,y)$ | = i th elastic mode normalized mode shape |
| | | $\phi'_i(x,y)$ | = $\partial \phi_i(x,y) / \partial x$, slope of $\phi_i(x,y)$ with respect to x , $1/\text{ft}$ |

Received July 6, 1976; presented as Paper 77-403 at the AIAA/ASME 18th Structures, Structural Dynamics, and Materials Conference, San Diego, Calif., March 21-23, 1977 (in bound Volume B of Conference papers); revision received April 26, 1977.

Index categories: Handling Qualities, Stability, and Control; Aerodynamics; Aeroelasticity and Hydroelasticity.

*Professor and Associate Head, School of Aeronautics and Astronautics, Associate Fellow AIAA.

†Graduate Student, School of Aeronautics and Astronautics; presently with Los Angeles Aircraft Division, Rockwell International. Member AIAA.

$\Xi_{im}(t)$ = i th elastic mode motion-dependent generalized force in z direction, ft/sec²
 $\Xi_{ig}(t)$ = i th elastic mode gust-induced generalized force in z direction, ft/sec²

Introduction

RECENT work with control-configured vehicles (CCV) and active control technology (ACT) has improved the performance, stability, and handling qualities of flexible airplanes and has opened up a new realm of design frontiers.¹ With increased size of present day airplanes, and with the increased utilization of lighter structures, the elastic behavior of these vehicles is becoming an appreciable influence in their handling and ride qualities. Because of the potential adverse effects of elastic mode interaction with the rigid-body dynamics, there is a need for a simplified method of modeling the dynamic aeroelastic equations of motion for use in preliminary control system design stages of new airplanes.

Usually, only calculated values of the rigid-body aerodynamic stability derivatives are available for the preliminary design from sources such as DATCOM,² and little, if any, information on the stability derivatives because of elastic modes is available then. However, calculated values of the symmetric and antisymmetric orthogonal elastic vibration mode shapes and natural frequencies are usually available at the preliminary design stage for use in equations-of-motion formulation.

We have developed a unique formulation of the longitudinal equations of motion for elastic airplanes that makes use of rigid-body aerodynamic stability derivatives and the elastic mode shapes and frequencies to describe the aerodynamic forces and moments caused by the elastic motion of the aircraft. The B-1 airplane is used as a model for accuracy verification.

Equations of Motion Formulation

The plunge and pitch rigid-body equations (short-period approximation) are included in what follows. The formulation of the small perturbation aerodynamic forces and moments is based on the local effective angle of attack, $\alpha(x,y,t)$, or effective plunge velocity, $w(x,y,t)$, where $w(x,y,t) = U_0 \alpha(x,y,t)$, and the local effective pitch rate, $\dot{\theta}(x,y,t)$. This is analogous to piston theory.

The elastic vibration characteristics are based on the usual approach of idealizing the structure to a flat plate in the xy plane, and the symmetric orthogonal free-free elastic vibration mode shapes $\phi_i(x,y)$ are functions of x and y coordinates in the x,y,z body axes system located at the center of gravity.³ The sign convention for the mode shapes, mode slopes, and generalized displacements is given in Fig. 1.

The two short-period and n elastic mode small perturbation equations of motion about a trim condition are given by Eq. (1):

$$\begin{aligned}
 \dot{w}(t) - U_0 \dot{\theta}(t) &= \int_y \int_x \frac{\partial^2 Z_w}{\partial x \partial y} w(x,y,t) dx dy \\
 &+ \int_y \int_x \frac{\partial^2 Z_q}{\partial x \partial y} \dot{\theta}(x,y,t) dx dy \\
 &+ Z_{\delta_e} \delta_e(t) + Z_w w_g(t) + Z_q q_g(t) \\
 \ddot{\theta}(t) &= \int_y \int_x \frac{\partial^2 M_w}{\partial x \partial y} w(x,y,t) dx dy + \int_y \int_x \frac{\partial^2 M_{\dot{w}}}{\partial x \partial y} \dot{w}(x,y,t) dx dy \\
 &+ \int_y \int_x \frac{\partial^2 M_q}{\partial x \partial y} \dot{\theta}(x,y,t) dx dy + M_{\delta_e} \delta_e(t) + M_w w_g(t) + M_q q_g(t) \\
 \ddot{\xi}_i(t) + 2\zeta_i \omega_i \dot{\xi}_i(t) + \omega_i^2 \xi_i(t) &= \Xi_{im}(t) + \Xi_{ig}(t) \quad (i=1,2,\dots,n)
 \end{aligned} \quad (1)$$

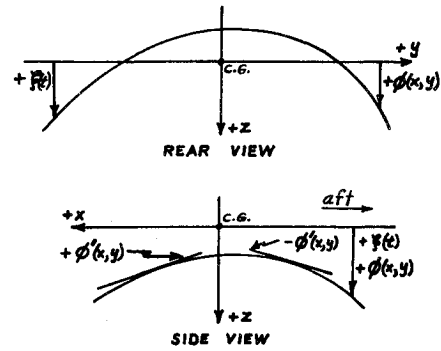


Fig. 1 Vertical bending sign convention.

Z_w , Z_{δ_e} , M_q , M_w , $M_{\dot{w}}$, and M_{δ_e} are the rigid-body dimensional aerodynamic stability derivatives defined in Eq. (2). $Z_{\dot{w}}$ is assumed to be negligible and is not included in Eq. (1). Implicit in the integrals of Eq. (1) is the assumption that aeroelastic deformation does not change significantly the stability derivatives of the rigid-body values. That is, flexibility corrections to the derivatives are neglected. The aerodynamics are assumed quasisteady (only zero frequency terms are retained in unsteady aerodynamic representations):

$$\begin{aligned}
 Z_q &= -\rho U_0 S c C_{L_q} / 4M & Z_{\delta_e} &= -\rho U_0^2 S C_{L_{\delta_e}} / 2M \\
 Z_w &= -\rho U_0 S (C_{L_\alpha} + C_D) / 2M & M_w &= \rho U_0 S c C_{m_\alpha} / 2I_y \\
 M_q &= \rho U_0 S c^2 C_{m_q} / 4I_y & M_{\delta_e} &= \rho U_0^2 S c C_{m_{\delta_e}} / 2I_y \\
 M_{\dot{w}} &= \rho S c^2 C_{m_{\dot{\alpha}}} / 4I_y
 \end{aligned} \quad (2)$$

The integral terms and the generalized force terms in Eq. (1) are functions of $w(x,y,t)$, and $\dot{\theta}(x,y,t)$, which can be approximated closely by Eqs. (3) and (4):

$$w(x,y,t) = w(t) + \sum_{i=1}^n \phi_i(x,y) \xi_i(t) - \sum_{i=1}^n U_0 \phi'_i(x,y) \xi_i(t) \quad (3)$$

$$\dot{\theta}(x,y,t) = \dot{\theta}(t) - \sum_{i=1}^n \phi'_i(x,y) \dot{\xi}_i(t) \quad (4)$$

The integral terms can be written as in Eqs. (5) and (6):

$$\begin{aligned}
 \int_y \int_x \frac{\partial^2 Z_w}{\partial x \partial y} w(x,y,t) dx dy + \int_y \int_x \frac{\partial^2 Z_q}{\partial x \partial y} \dot{\theta}(x,y,t) dx dy \\
 = Z_w w(t) + Z_q \dot{\theta}(t) + \sum_{i=1}^n [Z_{\xi_i} \xi_i(t) + Z_{\dot{\xi}_i} \dot{\xi}_i(t)]
 \end{aligned} \quad (5)$$

$$\begin{aligned}
 \int_y \int_x \frac{\partial^2 M_w}{\partial x \partial y} w(x,y,t) dx dy + \int_y \int_x \frac{\partial^2 M_{\dot{w}}}{\partial x \partial y} \dot{w}(x,y,t) dx dy \\
 + \int_y \int_x \frac{\partial^2 M_q}{\partial x \partial y} \dot{\theta}(x,y,t) dx dy = M_w w(t) + M_{\dot{w}} \dot{w}(t) \\
 + M_q \dot{\theta}(t) + \sum_{i=1}^n [M_{\xi_i} \xi_i(t) + M_{\dot{\xi}_i} \dot{\xi}_i(t) + M_{\ddot{\xi}_i} \ddot{\xi}_i(t)]
 \end{aligned} \quad (6)$$

The expressions for Z_{ξ_i} , $Z_{\dot{\xi}_i}$, M_{ξ_i} , $M_{\dot{\xi}_i}$, and $M_{\ddot{\xi}_i}$ are tabulated in Appendix A.

The expression for the motion-dependent generalized force term in the n elastic mode equations of motion of Eq. (1) is given by Eq. (7):

$$\Xi_{im}(t) = \frac{1}{\mathfrak{M}_i} \int_y \int_x \frac{\partial^2 Z(t)}{\partial x \partial y} \phi_i(x,y) dx dy \quad (7)$$

where

$$Z(t) = M \left[Z_w w(t) + Z_q \dot{\theta}(t) + \sum_{j=1}^n [Z_{\xi_j} \xi_j(t) + Z_{\xi_j} \dot{\xi}_j(t)] + Z_{\delta_e} \delta_e(t) \right] \quad (8)$$

and \mathfrak{M}_i is the i th mode generalized mass. Putting Eq. (8) into Eq. (7),

$$\begin{aligned} \Xi_{im}(t) = & F_{i_w} w(t) + F_{i_q} \dot{\theta}(t) + \sum_{j=1}^n [F_{i_{\xi_j}} \xi_j(t) \\ & + F_{i_{\dot{\xi}_j}} \dot{\xi}_j(t)] + F_{i_{\delta_e}} \delta_e(t) \end{aligned} \quad (9)$$

F_{i_w} , F_{i_q} , $F_{i_{\xi_j}}$, $F_{i_{\dot{\xi}_j}}$, $F_{i_{\delta_e}}$, and $F_{i_{w_g}}$ are tabulated in Appendix A.

The generalized force term because of C.G. referenced vertical gust velocities $w_g(t)$ and $q_g(t)$ is given by Eq. (10):

$$\begin{aligned} \Xi_{ig}(t) = & \frac{M}{\mathfrak{M}_i} \left[\int_y \int_x \frac{\partial^2 Z_w}{\partial x \partial y} \phi_i(x, y) dx dy \right] w_g(t) \\ & + \frac{M}{\mathfrak{M}_i} \left[\int_y \int_x \frac{\partial^2 Z_q}{\partial x \partial y} \phi_i(x, y) dx dy \right] q_g(t) \\ = & F_{i_{w_g}} w_g(t) + F_{i_{q_g}} q_g(t) \end{aligned} \quad (10)$$

Substituting Eqs. (5, 6, 9, and 10) into Eq. (1), Laplace transforming, and putting in matrix form yields Eq. (11), where four elastic modes ($n=4$) have been included explicitly:

$$\begin{bmatrix} s - Z_w & -U_0 s - Z_q s & -Z_{\xi_1} s - Z_{\xi_1} & -Z_{\xi_2} s - Z_{\xi_2} & -Z_{\xi_3} s - Z_{\xi_3} & -Z_{\xi_4} s - Z_{\xi_4} \\ -M_w s - M_w & s^2 - M_q s & -M_{\xi_1} s^2 - M_{\xi_1} s - M_{\xi_1} & -M_{\xi_2} s^2 - M_{\xi_2} s - M_{\xi_2} & -M_{\xi_3} s^2 - M_{\xi_3} s - M_{\xi_3} & -M_{\xi_4} s^2 - M_{\xi_4} s - M_{\xi_4} \\ -F_{1_w} & -F_{1_q} s & s^2 + (2\zeta_1 \omega_1 - F_{1_{\xi_1}}) s & -F_{1_{\xi_2}} s - F_{1_{\xi_2}} & -F_{1_{\xi_3}} s - F_{1_{\xi_3}} & -F_{1_{\xi_4}} s - F_{1_{\xi_4}} \\ & & + (\omega_1^2 - F_{1_{\xi_1}}) & & & \\ -F_{2_w} & -F_{2_q} s & -F_{2_{\xi_1}} s - F_{2_{\xi_1}} & s^2 + (2\zeta_2 \omega_2 - F_{2_{\xi_2}}) s & -F_{2_{\xi_3}} s - F_{2_{\xi_3}} & -F_{2_{\xi_4}} s - F_{2_{\xi_4}} \\ & & & + (\omega_2^2 - F_{2_{\xi_2}}) & & \\ -F_{3_w} & -F_{3_q} s & -F_{3_{\xi_1}} s - F_{3_{\xi_1}} & -F_{3_{\xi_2}} s - F_{3_{\xi_2}} & s^2 + (2\zeta_3 \omega_3 - F_{3_{\xi_3}}) s & -F_{3_{\xi_4}} s - F_{3_{\xi_4}} \\ & & & & + (\omega_3^2 - F_{3_{\xi_3}}) & s^2 + (2\zeta_4 \omega_4 - F_{4_{\xi_4}}) s \\ -F_{4_w} & -F_{4_q} s & -F_{4_{\xi_1}} s - F_{4_{\xi_1}} & -F_{4_{\xi_2}} s - F_{4_{\xi_2}} & -F_{4_{\xi_3}} s - F_{4_{\xi_3}} & + (\omega_4^2 - F_{4_{\xi_4}}) \end{bmatrix} \begin{bmatrix} w(s) \\ \theta(s) \\ \xi_1(s) \\ \xi_2(s) \\ \xi_3(s) \\ \xi_4(s) \end{bmatrix} = \begin{bmatrix} Z_{\delta_e} \\ M_{\delta_e} \\ F_{1_{\delta_e}} \\ F_{2_{\delta_e}} \\ F_{3_{\delta_e}} \\ F_{4_{\delta_e}} \end{bmatrix} \delta_e(s) + \begin{bmatrix} Z_w & Z_q \\ M_w & M_q \\ F_{1_{w_g}} & F_{1_{q_g}} \\ F_{2_{w_g}} & F_{2_{q_g}} \\ F_{3_{w_g}} & F_{3_{q_g}} \\ F_{4_{w_g}} & F_{4_{q_g}} \end{bmatrix} \begin{bmatrix} w_g(s) \\ q_g(s) \end{bmatrix} \quad (11)$$

Stability Derivatives Evaluation

Since elastic mode shape and slope data usually are given as a function of lumped mass stations, which themselves are given in xy coordinates, the double integrals in the terms of Appendix A can be represented conveniently as summations over incremental areas ($\Delta x \Delta y$) associated with each lumped mass point. Thus, it is necessary to develop methods for evaluating the following partial derivative terms at each point:

$$\frac{\partial^2 Z_{\delta_e}}{\partial x \partial y}, \frac{\partial^2 Z_w}{\partial x \partial y}, \frac{\partial^2 M_w}{\partial x \partial y}, \frac{\partial^2 M_{\dot{w}}}{\partial x \partial y}, \frac{\partial^2 M_q}{\partial x \partial y}, \frac{\partial^2 Z_q}{\partial x \partial y}.$$

Using Eq. (2), these become Eqs. (12-17):

$$\frac{\partial^2 Z_{\delta_e}}{\partial x \partial y} = \frac{-\rho U_0^2 S}{2M} \frac{\partial^2 C_{L_{\delta_e}}}{\partial x \partial y} \quad (12)$$

$$\frac{\partial^2 Z_w}{\partial x \partial y} = \frac{-\rho U_0 S}{2M} \left[\frac{\partial^2 C_{L_\alpha}}{\partial x \partial y} + \frac{\partial^2 C_D}{\partial x \partial y} \right] \quad (13)$$

$$\frac{\partial^2 M_w}{\partial x \partial y} = \frac{\rho U_0 S c}{2I_y} \frac{\partial^2 C_{m_\alpha}}{\partial x \partial y} \quad (14)$$

$$\frac{\partial^2 M_{\dot{w}}}{\partial x \partial y} = \frac{\rho S c^2}{4I_y} \frac{\partial^2 C_{m_\alpha}}{\partial x \partial y} \quad (15)$$

$$\frac{\partial^2 M_q}{\partial x \partial y} = \frac{\rho U_0 S c^2}{4I_y} \frac{\partial^2 C_{m_q}}{\partial x \partial y} \quad (16)$$

$$\frac{\partial^2 Z_q}{\partial x \partial y} = \frac{-\rho U_0 S c}{4M} \frac{\partial^2 C_{L_q}}{\partial x \partial y} \quad (17)$$

C_{L_α} , C_D , C_{m_α} , $C_{m_{\dot{\alpha}}}$, C_{m_q} , C_{L_q} , and $C_{L_{\delta_e}}$ are the total airplane rigid-body nondimensional stability derivatives referenced to the center of gravity, which are known constants for a trim flight condition. We need to determine the xy area distribution of these, i.e., the second partials in Eqs. (12-17).

For conventional-tailed airplanes, the lift curve slope can be approximated reasonably by

$$C_{L_\alpha} = C_{L_{\alpha W}} + C_{L_{\alpha HT}} \quad (18)$$

where $C_{L_{\alpha W}}$ and $C_{L_{\alpha HT}}$ are the wing and horizontal tail contributions. Fuselage lift is neglected as small. Methods for computing these can be found in Ref. 2. The tail contribution is about 10% of the total. Thus,

$$C_{L_{\alpha W}} = 0.9C_{L_\alpha} \quad C_{L_{\alpha HT}} = 0.1C_{L_\alpha} \quad (19)$$

A crude approximation, but one found to be adequate for this formulation, is to assume the derivatives to be distributed uniformly over the xy -plane representation of each component (i.e., wing, tail, fuselage). More accurate elliptical lift distributions were tried, but resulted in very little difference to characteristic roots obtained from Eq. (11) over that for the uniform distributions. Thus,

$$\frac{\partial^2 C_{L_\alpha}}{\partial x \partial y} = \begin{cases} 0 & \text{for fuselage stations } x(y=0) \\ C_{L_{\alpha W}}/S_W = (0.9/S_W)C_{L_\alpha} & \text{for wing stations } x,y \\ C_{L_{\alpha HT}}/S_{HT} = (0.1/S_{HT})C_{L_\alpha} & \text{for tail stations } x,y \end{cases} \quad (20)$$

where S_W and S_{HT} are wing and horizontal tail x,y planform areas. $C_D \ll C_{L_\alpha}$ and, therefore, C_D will be neglected in evaluation of Eq. (13).

Since $C_{L_{\delta_e}}$ is due only to elevator deflection,

$$\frac{\partial^2 C_{L_{\delta_e}}}{\partial x \partial y} = \begin{cases} C_{L_{\delta_e}}/S_{HT} & \text{for tail stations } x,y \\ 0 & \text{for wing and fuselage stations } x,y \end{cases} \quad (21)$$

Neglecting small effects caused by the fuselage,

$$C_{m_\alpha} = C_{m_{\alpha W}} + C_{m_{\alpha HT}} \quad (22)$$

$$\frac{\partial^2 C_{m_\alpha}}{\partial x \partial y} = \begin{cases} C_{m_{\alpha W}} & \text{for wing stations } x,y \\ C_{m_{\alpha HT}}/S_{HT} & \text{for tail stations } x,y \\ 0 & \text{for fuselage stations } x(y=0) \end{cases} \quad (23)$$

For the pitch damping derivatives,

$$C_{m_{\dot{\alpha}}} = C_{m_{\dot{\alpha} W}} + C_{m_{\dot{\alpha} HT}} \quad (24)$$

$$C_{m_q} = C_{m_{q WF}} + C_{m_{q HT}} \quad (25)$$

where WF indicates wing and fuselage combination.

$$\frac{\partial^2 C_{m_{\dot{\alpha}}}}{\partial x \partial y} = \begin{cases} C_{m_{\dot{\alpha} W}}/S_W & \text{for wing stations } x,y \\ C_{m_{\dot{\alpha} HT}}/S_{HT} & \text{for tail stations } x,y \\ 0 & \text{for fuselage stations } x(y=0) \end{cases} \quad (26)$$

$$\frac{\partial^2 C_{m_q}}{\partial x \partial y} = \begin{cases} C_{m_{q WF}}/(S_W + S_F) & \text{for wing and fuselage stations } x,y \\ C_{m_{q HT}}/S_{HT} & \text{for tail stations } x,y \end{cases} \quad (27)$$

Likewise,

$$\frac{\partial^2 C_{L_q}}{\partial x \partial y} = \begin{cases} C_{L_{q W}}/S_W & \text{for wing stations } x,y \\ C_{L_{q HT}}/S_{HT} & \text{for tail stations } x,y \\ 0 & \text{for fuselage stations } x(y=0) \end{cases} \quad (28)$$

Methods for estimating $C_{m_{\dot{\alpha} W}}$, $C_{m_{\dot{\alpha} HT}}$, $C_{m_{q WF}}$, $C_{m_{q HT}}$, $C_{L_{q W}}$, and $C_{L_{q HT}}$ are given in Refs. 2 and 4. Knowing the airplane elastic mode shapes, slopes, and six rigid-body total-airplane stability derivatives, all of the terms in Appendix A, and thus the coefficients in Eq. (11), can be computed.

Verification with B-1 Airplane Dynamics

To verify the accuracy of the unique formulation of elastic airplane small perturbation dynamic equations of motion developed in the foregoing, the terms in Eq. (11) are calculated for the B-1 at a sea level, Mach 0.85 flight condition and compared with the corresponding terms in equations provided by Rockwell,^{5,6} which were generated by other methods.

As an example of how the double integrals are evaluated, consider the term for the generalized force of the second elastic mode because of the third mode. From Appendix A, it is

$$F_{2\epsilon_3} = \frac{-U_0 M}{9\pi_2} \int_y \int_x \frac{\partial^2 Z_w}{\partial x \partial y} \phi_2(x,y) \phi_3'(x,y) dx dy \quad (29)$$

By summing over n mass stations, the term becomes

$$F_{2\epsilon_3} = \frac{-U_0 M}{9\pi_2} \sum_{i=1}^n \left(\frac{\partial^2 Z_w}{\partial x \partial y} \right)_i \phi_2(i) \phi_3'(i) (\Delta x \Delta y)_i \quad (30)$$

The $(\Delta x \Delta y)_i$ term is the area associated with each lumped mass point. $\phi_2(i)$ and $\phi_3'(i)$ are the values of the second mode shape and third mode slope in the chordwise x direction at the i th mass point. $(\partial^2 Z_w / \partial x \partial y)_i$ has three constant values; one for fuselage stations, one for wing stations, and one for horizontal tail stations. $C_{L_\alpha} = 3.94$ for this B-1 flight condition. Wing and tail areas are $S = S_W = 1946 \text{ ft}^2$, $S_{HT} = 502 \text{ ft}^2$. From Eq. (20),

$$\frac{\partial^2 C_{L_\alpha}}{\partial x \partial y} = \begin{cases} 0 & \text{fuselage stations} \\ 18.22 \times 10^{-4} / \text{ft}^2 & \text{wing stations} \\ 7.85 \times 10^{-4} / \text{ft}^2 & \text{tail stations} \end{cases} \quad (31)$$

From Eq. (13), with C_D neglected as small,

$$\left(\frac{\partial^2 Z_w}{\partial x \partial y} \right)_i = \begin{cases} 0 & \text{fuselage stations} \\ -5.708 \times 10^{-4} / \text{ft}^2\text{-sec} & \text{wing stations} \\ -2.213 \times 10^{-4} / \text{ft}^2\text{-sec} & \text{tail stations} \end{cases} \quad (32)$$

The calculation of Eq. (30) gives $F_{2\epsilon_3} = 5.8459$, which compares with 6.6257 obtained from Rockwell's formulation of the equations.

All of the other coefficients in Eq. (11) were evaluated similarly and are tabulated, along with the values from Rockwell's B-1 equations of motion, in Appendix B. Approximately 80% of the terms show acceptable agreement with the B-1 data. In view of the highly approximate nature of the formulation, this is reasonable confirmation of the validity of the method.

A further check was made by comparing the roots of the characteristic equations for the B-1 data and this formulation by expanding the determinant of the 6×6 matrix of polynomials and coefficients in Eq. (11). The coupled

Table 1 Frequencies and damping ratios

| B-1 data | | Present method | |
|-----------|---------|----------------|---------|
| Frequency | Damping | Frequency | Damping |
| 2.868 | 0.489 | 2.935 | 0.513 |
| 13.298 | 0.053 | 13.694 | 0.034 |
| 21.375 | 0.031 | 21.236 | 0.025 |
| 22.020 | 0.020 | 22.054 | 0.020 |
| 22.480 | 0.206 | 25.373 | 0.233 |

frequencies in rad/sec and damping ratios were calculated for each pair of complex roots. The comparisons are shown in Table 1. It is evident from the data in this table that the new formulation of the equations of motion is surprisingly accurate considering the level of approximations made. The four symmetric elastic modes of the B-1 had free-free undamped natural frequencies of 13.591, 14.123, 21.198, and 22.055 rad/sec. All had 0.02 structural damping ratios. The first line of numbers in Table 1 corresponds to the short-period frequency and damping ratio.

Conclusions

This method of formulation of the longitudinal small perturbation equations of motion for elastic airplanes allows the expression of aerodynamic forces and moments, because of elastic vibration, in terms of rigid-body aerodynamic stability derivatives. Thus, it is potentially a useful preliminary design tool for airplane stability and control, handling and ride qualities, and control system design studies.

The good accuracy of the method was established by comparison with more accurate data for the B-1 airplane. The lack of complete information on the planform geometry of the B-1 and our having analytically to calculate mode slopes by curve fits from the mode shape data, may account for some of what differences appear in the term-by-term comparisons in Appendix B. Therefore, the new method is possibly even more accurate than this one example comparison indicates. We have completed a similar formulation for the lateral-directional dynamics with the antisymmetric elastic modes included.⁷

Appendix A: Equation (11) Coefficients

$$Z_{\xi_i} = -U_0 \int_y \int_x \frac{\partial^2 Z_w}{\partial x \partial y} \phi'_i(x, y) dx dy$$

$$Z_{\xi_i} = \int_y \int_x \frac{\partial^2 Z_w}{\partial x \partial y} \phi_i(x, y) dx dy - \int_y \int_x \frac{\partial^2 Z_q}{\partial x \partial y} \phi'_i(x, y) dx dy$$

$$M_{\xi_i} = \int_y \int_x \frac{\partial^2 M_w}{\partial x \partial y} \phi_i(x, y) dx dy$$

$$M_{\xi_i} = \int_y \int_x \left\{ \frac{\partial^2 M_w}{\partial x \partial y} \phi_i(x, y) - \left[U_0 \frac{\partial^2 M_w}{\partial x \partial y} + \frac{\partial^2 M_q}{\partial x \partial y} \right] \phi'_i(x, y) \right\} dx dy$$

$$M_{\xi_i} = -U_0 \int_y \int_x \frac{\partial^2 M_w}{\partial x \partial y} \phi'_i(x, y) dx dy$$

$$F_{i_w} = \frac{M}{\mathfrak{M}_i} \int_y \int_x \frac{\partial^2 Z_w}{\partial x \partial y} \phi_i(x, y) dx dy = F_{i_{wg}}$$

$$F_{i_q} = \frac{M}{\mathfrak{M}_i} \int_y \int_x \frac{\partial^2 Z_q}{\partial x \partial y} \phi_i(x, y) dx dy = F_{i_{qg}}$$

$$F_{i_{\xi_j}} = -\frac{U_0 M}{\mathfrak{M}_i} \int_y \int_x \frac{\partial^2 Z_w}{\partial x \partial y} \phi_i(x, y) \phi'_j(x, y) dx dy$$

$$F_{i_{\xi_j}} = \frac{M}{\mathfrak{M}_i} \int_y \int_x \left\{ \frac{\partial^2 Z_w}{\partial x \partial y} \phi_i(x, y) \phi_j(x, y) - \frac{\partial^2 Z_q}{\partial x \partial y} \phi_i(x, y) \phi'_j(x, y) \right\} dx dy$$

$$F_{i_{\delta_e}} = \frac{M}{\mathfrak{M}_i} \int_y \int_x \frac{\partial^2 Z_{\delta_e}}{\partial x \partial y} \phi_i(x, y) dx dy$$

Appendix B: Coefficient Values

| Term | From B-1 Equations | From Present Method |
|-----------------|--------------------------|---------------------------|
| F_{1_w} | -0.77480 | -0.69335 |
| F_{2_w} | 1.3590 | 1.4180 |
| F_{3_w} | 0.80586 | 0.81559 |
| F_{4_w} | 1.7902×10^{-3} | 1.8274×10^{-3} |
| Z_{ξ_1} | -0.20177 | -0.01798 |
| Z_{ξ_2} | 2.4702 | 1.9202 |
| Z_{ξ_3} | 0.14486 | 0.15373 |
| Z_{ξ_4} | -4.7412×10^{-3} | 0.11254 |
| Z_{ξ_1} | -8.4911 | -6.7715 |
| Z_{ξ_2} | 90.322 | 103.32 |
| Z_{ξ_3} | 4.3792 | -1.3083 |
| Z_{ξ_4} | -4.1323 | -5.3236 |
| M_{ξ_1} | 0 | -0.72033×10^{-4} |
| M_{ξ_2} | 0 | -3.6129×10^{-4} |
| M_{ξ_3} | 0 | 1.4315×10^{-4} |
| M_{ξ_4} | 0 | 0.06947×10^{-4} |
| M_{ξ_1} | -7.5404×10^{-3} | -10.823×10^{-3} |
| M_{ξ_2} | 50.866×10^{-3} | 2.9502×10^{-3} |
| M_{ξ_3} | 7.0361×10^{-3} | 16.427×10^{-3} |
| M_{ξ_4} | -2.0060×10^{-3} | -3.0665×10^{-3} |
| M_{ξ_1} | -0.18849 | -0.04194 |
| M_{ξ_2} | -0.07903 | -0.01592 |
| M_{ξ_3} | 0.20945 | 0.07459 |
| M_{ξ_4} | -0.09381 | -0.01065 |
| $F_{1_{\xi_1}}$ | -0.86630 | -1.1180 |
| $F_{1_{\xi_2}}$ | -0.28286 | 17.818 |
| $F_{1_{\xi_3}}$ | 0.91557 | -0.07921 |
| $F_{1_{\xi_4}}$ | -0.19759 | -0.69559 |
| $F_{2_{\xi_1}}$ | 7.2681 | -31.795 |
| $F_{2_{\xi_2}}$ | -15.897 | 643.69 |
| $F_{2_{\xi_3}}$ | 61.886 | 9.640 |
| $F_{2_{\xi_4}}$ | 20.894 | -18.803 |
| $F_{2_{\xi_1}}$ | 0.23360 | 0.34121 |
| $F_{2_{\xi_2}}$ | -8.2949 | -10.334 |
| $F_{2_{\xi_3}}$ | 0.11424 | 0.00560 |
| $F_{2_{\xi_4}}$ | 0.11188 | 0.11583 |
| $F_{2_{\xi_1}}$ | 14.002 | 18.740 |
| $F_{2_{\xi_2}}$ | -306.000 | -415.280 |
| $F_{2_{\xi_3}}$ | 6.6257 | 5.8459 |
| $F_{2_{\xi_4}}$ | 11.211 | 14.696 |
| $F_{3_{\xi_1}}$ | -0.12060 | -0.010897 |
| $F_{3_{\xi_2}}$ | 3.7684 | 0.04020 |
| $F_{3_{\xi_3}}$ | -0.42578 | -0.18203 |
| $F_{3_{\xi_4}}$ | -0.25330 | -0.11246 |
| $F_{3_{\xi_1}}$ | 7.0455 | 2.6015 |
| $F_{3_{\xi_2}}$ | 33.993 | -15.509 |
| $F_{3_{\xi_3}}$ | -7.9516 | -1.5492 |
| $F_{3_{\xi_4}}$ | 3.4837 | 2.0596 |

| | | |
|-------------------|--------------------------|---------------------------|
| $F_{4\epsilon_1}$ | -3.2701×10^{-4} | -2.9290×10^{-4} |
| $F_{4\epsilon_2}$ | 24.031×10^{-4} | 25.469×10^{-4} |
| $F_{4\epsilon_3}$ | -2.7776×10^{-4} | -3.4422×10^{-4} |
| $F_{4\epsilon_4}$ | -4.0417×10^{-4} | -4.2249×10^{-4} |
| $F_{4\epsilon_1}$ | 1.6305×10^{-2} | -0.04974×10^{-2} |
| $F_{4\epsilon_2}$ | -9.7878×10^{-2} | 3.6896×10^{-2} |
| $F_{4\epsilon_3}$ | 0.70767×10^{-2} | 0.24563×10^{-2} |
| $F_{4\epsilon_4}$ | 1.3340×10^{-2} | 0.18614×10^{-2} |
| $F_{1\delta_e}$ | -22.296×10^2 | -15.978×10^2 |
| $F_{2\delta_e}$ | -2.1741×10^2 | -1.5347×10^2 |
| $F_{3\delta_e}$ | 6.1537×10^2 | 4.3685×10^2 |
| $F_{4\delta_e}$ | 0.11048 | 0.06489 |
| F_{1q} | -135.494 | -38.298 |
| F_{2q} | 23.123 | -5.593 |
| F_{3q} | 50.187 | 6.847 |
| F_{4q} | 0.0313 | -5.885 |

Acknowledgment

This research was supported by the Vehicle Dynamics and Control Division of the NASA Dryden Flight Research Center under grant NSG 4003.

References

- ¹Rediess, H. A. (ed.), *Proceedings of the NASA Symposium on Advanced Control Technology and Its Potential for Future Transport Aircraft*, Los Angeles, Calif., NASA TMX-3409, Aug. 1976.
- ²Ellison, D. E., Finck, R. D., and Hoak, D. E., *USAF Stability and Control Datcom*, Wright-Patterson Air Force Base, Ohio, Oct. 1960 (revised Aug. 1968).
- ³Bisplinghoff, R. L., Ashley, H., and Halfman, R. L., *Aeroelasticity*, Addison-Wesley, Reading, Mass., 1955, pp. 106-114.
- ⁴Roskam, J., "Methods for Estimating Stability and Control Derivatives of Conventional Subsonic Airplanes," Roskam Aviation and Engineering Corp., Lawrence, Kansas, 1971.
- ⁵Wykes, J. H., "B-1 Flexible Vehicle Equations of Motion for Ride Quality, Terrain Following, and Handling Quality Studies," Rockwell International B-1 Division, Los Angeles, Calif., TFD-71-430-1, Jan. 1973.
- ⁶Freeman, R. C. and Rozsa, T. I., "Basic Modal Data Package for -55B Mid-Penetration Weight 65 Degree Wing Sweep," Rockwell International B-1 Division, Los Angeles, Calif., TFD-73-362, March 1973.
- ⁷Swaim, R. L. and Staab, G. H., "Prediction of Elastic-Airplane Lateral Dynamics from Rigid-Body Aerodynamics," AIAA Paper 77-1125, Hollywood, Fla., Aug. 1977.

From the AIAA Progress in Astronautics and Aeronautics Series . . .

INSTRUMENTATION FOR AIRBREATHING PROPULSION—v. 34

Edited by Allen Fuhs, Naval Postgraduate School, and Marshall Kingery, Arnold Engineering Development Center

This volume presents thirty-nine studies in advanced instrumentation for turbojet engines, covering measurement and monitoring of internal inlet flow, compressor internal aerodynamics, turbojet, ramjet, and composite combustors, turbines, propulsion controls, and engine condition monitoring. Includes applications of techniques of holography, laser velocimetry, Raman scattering, fluorescence, and ultrasonics, in addition to refinements of existing techniques.

Both inflight and research instrumentation requirements are considered in evaluating what to measure and how to measure it. Critical new parameters for engine controls must be measured with improved instrumentation. Inlet flow monitoring covers transducers, test requirements, dynamic distortion, and advanced instrumentation applications. Compressor studies examine both basic phenomena and dynamic flow, with special monitoring parameters.

Combustor applications review the state-of-the-art, proposing flowfield diagnosis and holography to monitor jets, nozzles, droplets, sprays, and particle combustion. Turbine monitoring, propulsion control sensing and pyrometry, and total engine condition monitoring, with cost factors, conclude the coverage.

547 pp. 6 x 9, illus. \$14.00 Mem. \$20.00 List

TO ORDER WRITE: Publications Dept., AIAA, 1290 Avenue of the Americas, New York, N. Y. 10019